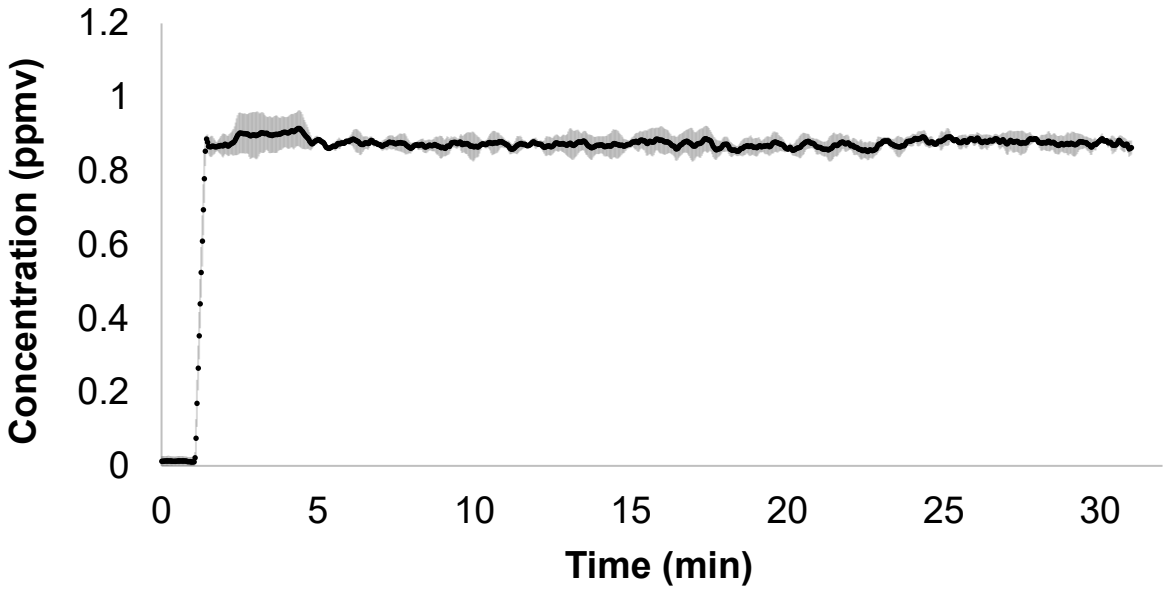

Supplementary Fig. 1 | Ozone concentration in the duct 15 cm downstream of the ESP-SDBD filter outlet during ESP collection operation with 1 m/s airflow. The average steady-state ozone concentration was 0.876 ppmv. The lightly shaded error bars represent the standard deviation over triplicate experiments.

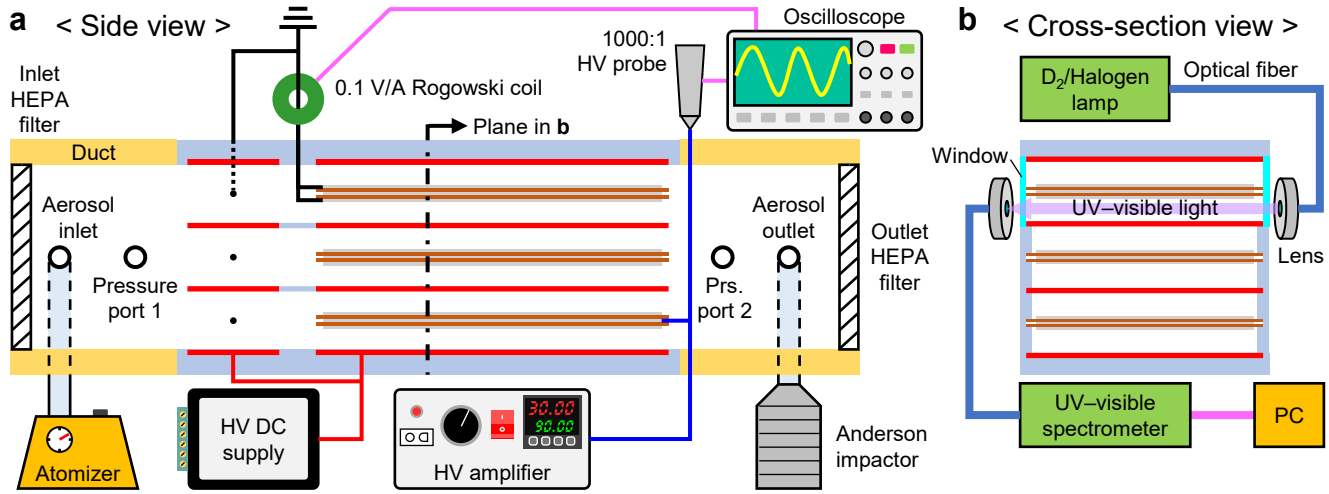

Supplementary Fig. 2 | Experiment setup. a Experiment setup for airborne bacteria collection and collected bacteria inactivation experiments. The ESP-SDBD filter, electrical power supplies and diagnostics, and bacterial aerosol generation and collection systems are illustrated. **b** Experiment setup for *in-situ* ozone concentration measurement using broadband UV–visible absorption spectroscopy.

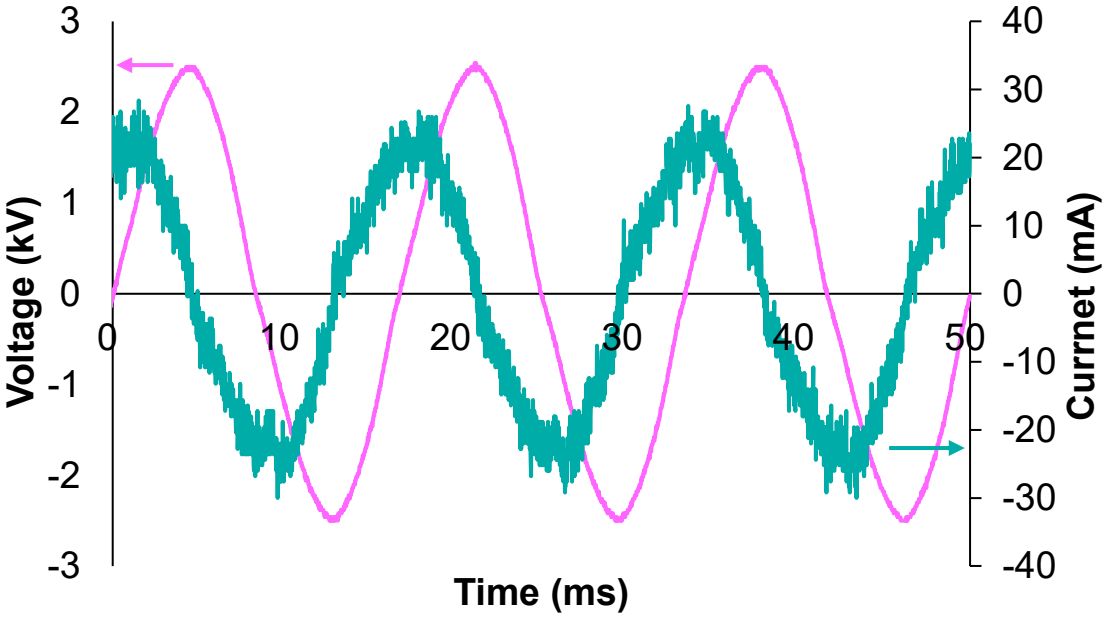

Supplementary Fig. 3 | Voltage and current waveforms of the SDBD units.

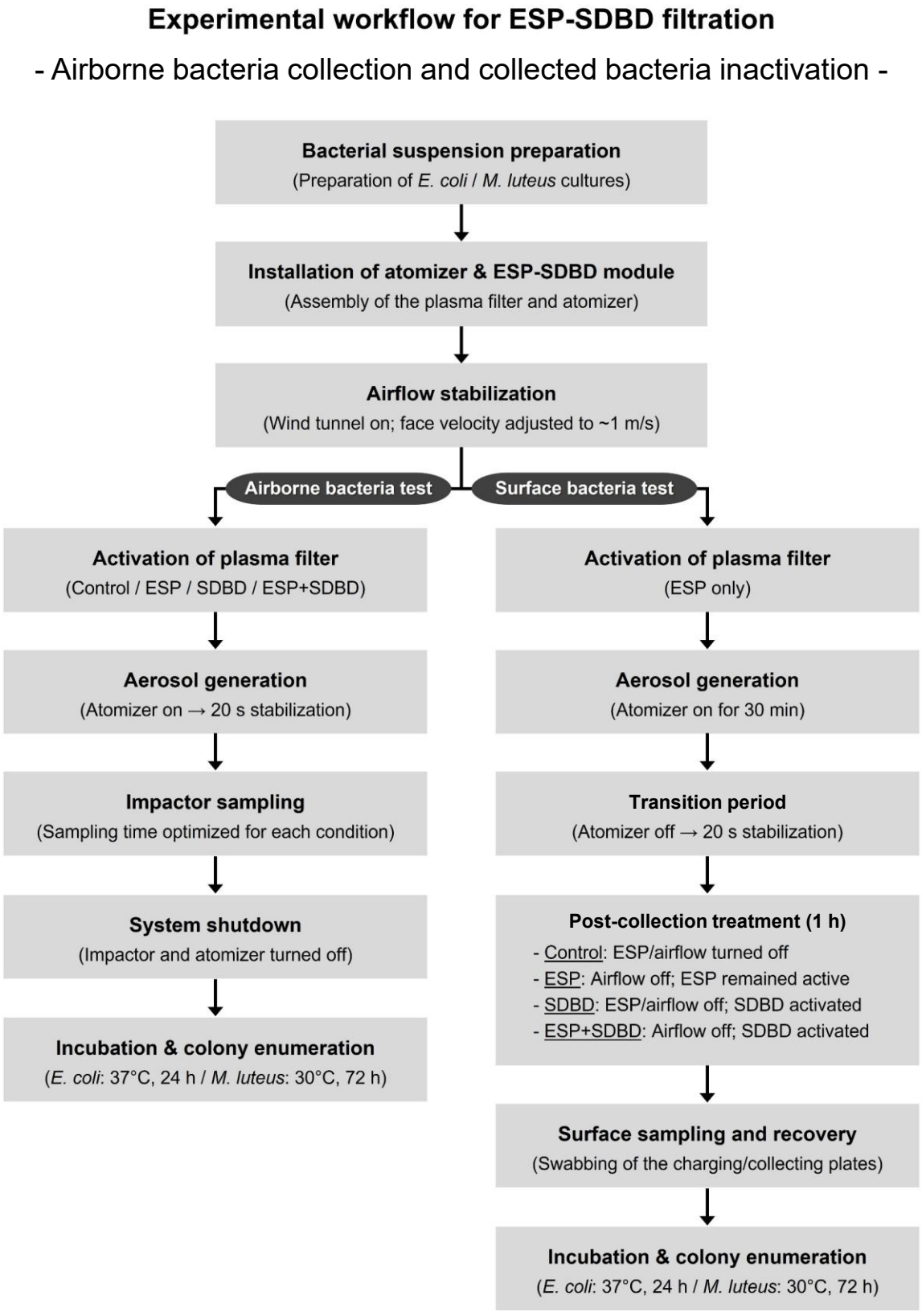

Supplementary Fig. 4 | Flowchart for procedure for airborne bacteria collection and collected bacteria inactivation experiments.

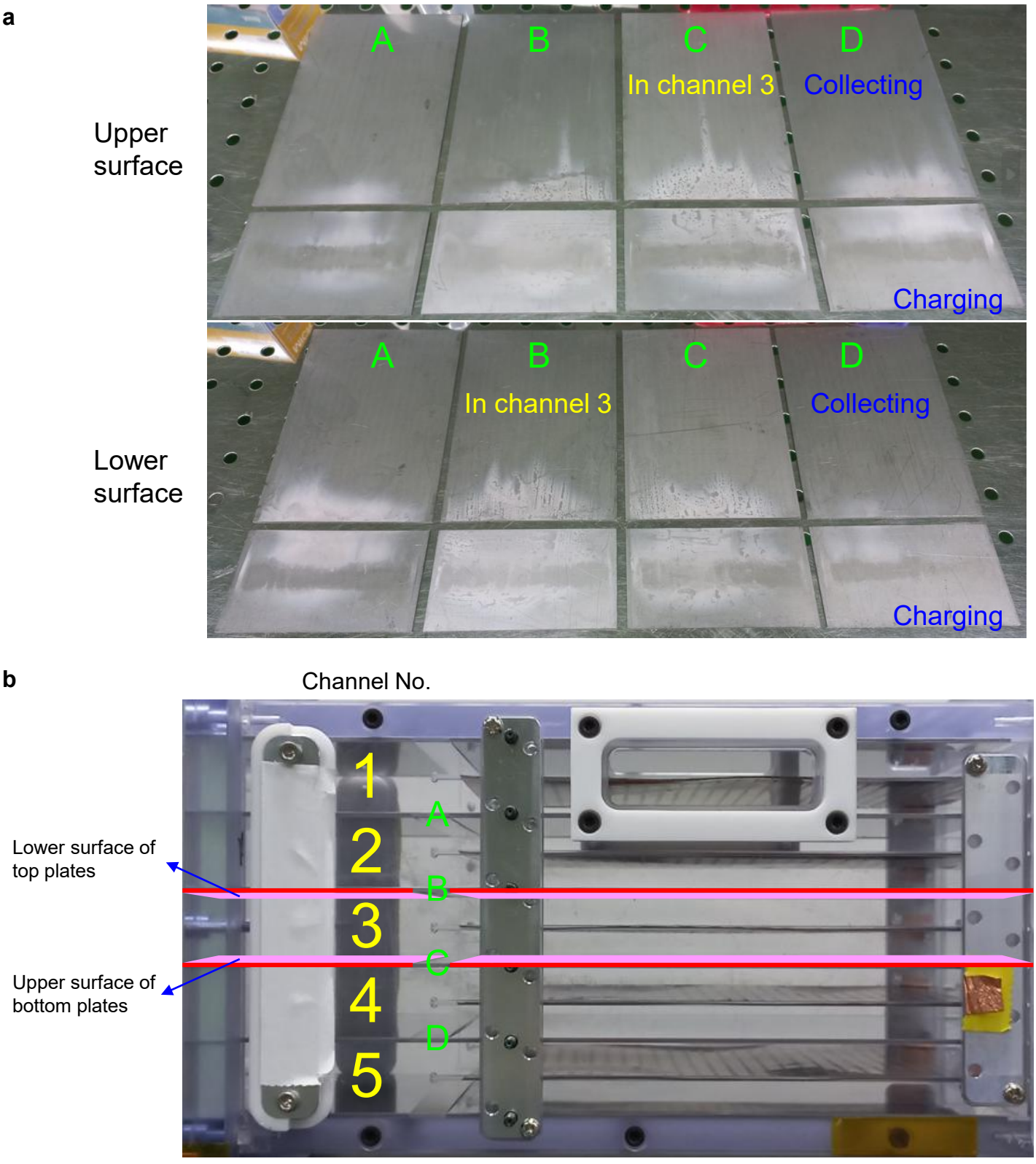

Supplementary Fig. 5 | Collection of airborne bacterial aerosols on the charging and collecting plates. a Spatial distribution of electrostatically collected bacterial aerosols on the charging and collecting plates of the ESP-SDBD filter. The spatial distribution of collection is visually observable by the white salt left on the plates that were dissolved in the aerosolized saline solution carrying the bacteria. **b** The location of the surfaces of the charging and collecting plates facing into the central channel 3 which surfaces were sampled for the quantification of surface-attached bacteria.

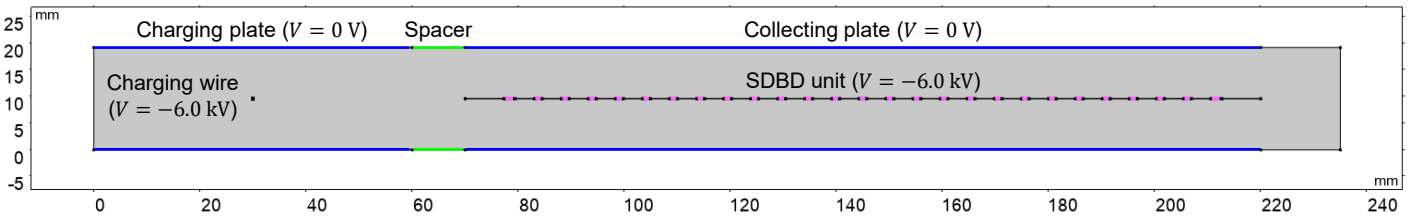

Supplementary Fig. 6 | Domain of a single ESP-SDBD filter channel for corona discharge and associated electric wind simulation. Although the experiments were performed with the charging wire and SDBD unit electrode surfaces at ground potential ($V = 0$ V) and the charging and collecting plates at high positive potential ($V = +6.0$ kV), the electric potential values were shifted by -6.0 kV in the simulation to improve the convergence of the simulation. This did not affect the simulation results because the electric potential reference point can be chosen arbitrarily.

	Outflowing airstream bacterial density (log CFU/m^3)		Airborne bacterial reduction by ESP operation	
	Control	SDBD operation	log CFU/m^3	Collection efficiency (%)
E. coli	5.86±0.03	5.98±0.06	4.61	99.998
M. luteus	5.50±0.01	5.59±0.04	4.25	99.994

Supplementary Table 1 | Outflowing airstream bacterial densities and airborne bacterial reduction by ESP operation. The airborne bacterial reduction by ESP operation was obtained by subtracting the LOD of 1.25 log CFU/m^3 from the corresponding control group value, due to airborne bacteria being not detected (ND) in the outflowing airstream during ESP operation. The errors represent the standard deviation over triplicate experiments. Data in this table corresponds to data in main text Fig. 2b–c.

Operation mode	Charging plates	Collecting plates
ESP	1.57±0.34	2.33±0.14
SDBD	3.20±0.40	2.38±0.27
ESP+SDBD	3.88±0.42	3.61±0.23

Supplementary Table 2 | Average log reduction of *M. luteus* collected on the charging and collecting plates For the ESP+SDBD results, the LOD of 0.159 CFU/cm^2 for the charging plates and 0.0635 CFU/cm^2 for the collecting plates were substituted for the not detected (ND) values when calculating the average. Data in this table corresponds to data in main text Fig. 2d.